SAMODEJNA RAZMEJITEV VODNIH TELES Z UPORABO PODATKOV CORINE IZ DALJINSKO ZAZNANIH SLIK

AUTOMATIC DELINEATION OF WATER BODIES USING CORINE DATA FROM REMOTELY SENSED IMAGES

Dilek Küçük Matci

UDK: 004.652:528.8
Klasifikacija prispevka po COBISS.SI: 1.01
Prispelo: 7. 2. 2022
Sprejeto: 8. 8. 2022

DOI: 10.15292/geodetski-vestnik.2022.03.387-402
SCIENTIFIC ARTICLE
Received: 7. 2. 2022
Accepted: 8. 8. 2022

IZVLEČEK

Vodni viri so ključnega pomena za obstoj življenja, zaradi česar je pomembno, da jih kartiramo. Z uspešno analizo daljinsko zaznanih slik lahko pridobimo zanesljive informacije za raziskave vode, vendar je postopek zapleten in poskrbeti moramo, da na ustvarjene karte ne vplivajo sence, oblaki ali drugi šumi. Poleg tega je treba uspešno preslikati vse vrste voda na različnih geografskih območjih. Pomembno je tudi, da je uporabljena metoda praktična, da lahko znanstveniki, ki niso slikovni analitiki, uporabljajo širok nabor podatkov, ki jih zagotavljajo satelitske slike.

V prispevku je predlagan nov algoritem za ekstrakcijo vodnega telesa iz posnetkov Landsat. Pri tej metodi se podatki Corine uporabljajo kot pomožni podatki za samodejno ustvarjanje učnih podatkov. Za testiranje predlagane metode se uporabljajo štiri študijska področja z različnimi značilnostmi iz različnih delov sveta. Dobljene rezultate primerjamo z drugimi samodejnimi metodami razvrščanja.

ABSTRACT

Water resources is crucial for the continuity of life. Therefore, mapping water resources is required. Successful analysis of remotely sensed images can provide reliable information for water researches. However, it is very complex process to ensure that the maps created are not affected by shadows, cloud or other noise. In addition, it is necessary to successfully map all water types in various geographies. It is important that the method used is practical so that scientists who are not image analysts can use the large data pool provided by satellite images.

In this paper, a novel algorithm for water body extraction from Landsat imagery is proposed. In this method, Corine data are used as auxiliary data to automatically generate training data. Four study areas with different characteristics, from different parts of the world, are used to test the proposed method. The results obtained are compared with other automatic classification methods.

KLJUČNE BESEDE

daljinsko zaznavanje, obdelava slik, vodno telo, reka, podatki Corine

KEY WORDS

remote sensing, image processing, water body, river, corine data

1 INTRODUCTION

Climate change and rapid, uncontrolled urbanization in recent years have affected the distribution and quality of water areas (Franczyk and Chang, 2009; Huong and Pathirana, 2013). Sustaining a healthy environment, climate and agriculture depend on the protection of water resources. Regular monitoring of water resources and the identifiying changes are the first steps towards conservation of resources. On the other hand, it is necessary to monitor water bodies in order to reveal floods and their effects on the environment as a result of the storms and excessive precipitation which are a result of the changing climate (Huong and Pathirana, 2013).

With the rapid development of technology, remotely sensed images have begun to provide data about environmental changes in many areas. In the past years, various water body extraction studies have been carried out using remotely sensed images (Chen et al., 2020; Feng et al., 2016; Monegaglia et al., 2018; Rad et al., 2021; Somasundaram et al., 2020). In one of these studies, an inland water body dataset was created using Landsat satellite images. Landsat images are used in another water extraction study, surface water area extraction has been carried out by using learning vector quantization (LVQ) methods (Somasundaram et al., 2020). Similarly, Landsat images were used to test theproposed method (Monegaglia et al., 2018). In another study a novel neural network method for water body extraction method was proposed. To evaluate this proposed method, ZY-3, GF-1, and GF-2 multispectral images were used (Chen et al., 2020).

The water index, which is used to identify water areas, is a simple and effective method of identifying surface water bodies by separating the signals of water from other surface classes with the band ratio method. The normalized difference water index (NDWI) based on extracting green and near infrared (NIR) bands from multispectral bands has been proposed (McFeeters, 2013). The modified normalized difference water index (MNDWI) has been proposed to suppress background residential areas, while eliminating water areas (Hanqiu Xu, 2006). Recently, the Augmented Normalized Difference Water Index has been proposed to extract water bodies from Landsat images (Rad et al., 2021). Other water indices such as the automated water extraction index (AWEI), all band water index (ABWI) and multi-band water index (MBWI) have been proposed using other bands in multispectral images (Feyisa et al., 2014; Wang et al., 2018; Xiong et al., 2018).

One of the other water extraction approaches is supervised classification approaches. For example, a water and urban land use map was prepared is a random forest (RF) classifier (Chen et al., 2018). Also, two machine learning frameworks (pixel based and object based) have been proposed to determine water types (Huang et al., 2015). The monthly changes in the water surface area of Lake were determined in another study using Landsat and Sentinel 1 images and the Otsu method (Jingzhe Wang et al., 2019). Using different satellite images, spectral indices, and thresholds, the spatial and volumetric changes of the Aral Lake between 1960 and 2018 have been determined in one of the recent studies (Yang et al., 2020).

Unsupervised classification methods are frequently used in the literature for the extraction of water areas. In a study conducted in Sri Lanka, the Learning Vector Quantization (LVQ) method was used to extract the water area. The obtained results were compared with other state of the art methods such as support vector machine, K-nearest neighbor, discriminant analysis, combination of modified normalized difference water index and modified fuzzy clustering method, and K-means methods. The results of the

study indicated that LVQ performed well in detecting all water types with fewer training samples (Somasundaram et al., 2020). In another study, LVQ was used to extract water areas from Landsat 4 images (Wang and Zhu, 2003). In a study proposed to extract water regions in mountainous areas, the image was first classified with K-Means, and these classes were used as masks (Gao et al., 2016). High resolution Dem and K-Means were used in a study to extract valley and channel networks (Hooshyar et al., 2016).

When these studies are examined, supervised classification generally gives higher accuracy results, compared to unsupervised classification or water indices (Jiang et al., 2018). However, creating separate training data for each classification in the supervised classification process is laborious and time-consuming. In addition, the accuracy of the training data directly affects the results (Foody and Mathur, 2004; Matci and Avdan, 2020).

Corine data have been created for the purpose of monitoring natural resources, and prepared in line with the criteria determined by the European Environment Agency (Corine, 2019). The European Corine land cover mapping scheme has a 100m resolution and includes 44 land cover and land use classes. These data are used in various studies such as the determination of the changes in land cover classes, the creation of population density maps, the spatial interpolation of air pollution measurements, and the determination of urban heat islands (Dabija et al., 2021; Dzieszko, 2014; Gallego and Peedell, 2001; Janssen et al., 2008; Kucsicsa et al., 2019; Stathopoulou and Cartalis, 2007; Waltner et al., 2020). In a study conducted using this data, the effectiveness of satellite image classification, according to the Corine land cover guidelines, was examined. Training data were collected by randomly selecting samples of pixels falling within the Corine land classes (Dabija et al., 2021). In another study, Corine data were used to reveal the main land-use and land-cover change (LUCC) patterns in the Poznań Lakeland mesoregion (Dzieszko, 2014). In a study to identify and predict land cover change in Romania, Corine data was used in conjunction with the existing land use/cover model(Kucsicsa et al., 2019). In a study conducted in Greece, an urban heat island extraction study was conducted and Corine data were used together with Landsat 7 images(Stathopoulou and Cartalis, 2007).

The Corine data were used in another study to improve the mapping of population density that the European Commission could use at the commune level (Gallego and Peedell, 2001). In another study, Corine data were used to model air pollution data(Janssen et al., 2008). Corine data were used in a study to evaluate changes in soil erosion potential caused by changes in land use and land cover based on Land Cover data in Hungary (Waltner et al., 2020).

This study uses a fully automate water extraction approach, from satellite images, using data. The method uses a training data collection system based on the Corine data. With the training data prepared in this way, the water bodies in selected areas outside the Corine region were also successfully extracted from the Landsat Images. In order to test the method developed, images of regions in Canada, Guinea, Zhengzhou and Tibetan were used, and the water bodies in these areas were automatically mapped. The results obtained reveal the potential of the proposed method.

2 MATERIALS AND METHODS

The materials and methods used in the study are presented under the following sub-headings.

2.1 Satellite Imagery

Launched on February 11, 2013, Landsat-8 collection includes two sensors, the Operational Land Imager (OLI) and Thermal Infrared Sensors (TIRS). Landsat-8 OLI images were used in the study. The bands of the Landsat-8 satellite used in the study are given in Table1.

Table 1: Specifications of Images Used in the Study

Satellite	Band Name	Resolution (m)	Wavelength(nm)
Landsat 8	Blue	30	483
	Green	30	560
	Red	30	660
	NIR	30	865
	SWIR	30	1650
	SWIR	30	2220

In the study, 30m resolution Landsat images were used. The acquired dates of the images are given in Table2.

Table 2: Acquisition Date of Used Images

	Study Area	Specification of the Area	Landsat 8
Training	Turkey, Greece, Sweden, UK, France	Turkey: Sea, Lake, Urban areas, river, Agricultural areas Greece: Sea, Fr: Muddy canal, Sweden: Surrounded by the trees.	Mean of images acquired between 01.01.2021-09.12.2021
Classification	Loughborough Lake, Canada	It has different depths and is surrounded by trees.	24.08.2021
	Guinea Region	Muddy and the shores are covered with rhizophoraceae mangroves	03.06.2021
	Lake yamzho Yumco, Tibet	The selected area is surrounded by snow-capped mountains	28.01.2021 04.02.2021
	Yellow River Zhengzhou,China	The selected area has urban areas, water bodies, mostly turbid rivers, artificial channels, artificial lakes, reservoirs and ponds.	02.10.2021

2.2 Study Areas

In order to test the proposed method, images of the regions given in Figure 1 were chosen. The reason for choosing these study regions is that the proposed method can be evaluated in various geographical conditions (mountainous, delta, urban, with and without vegetation).

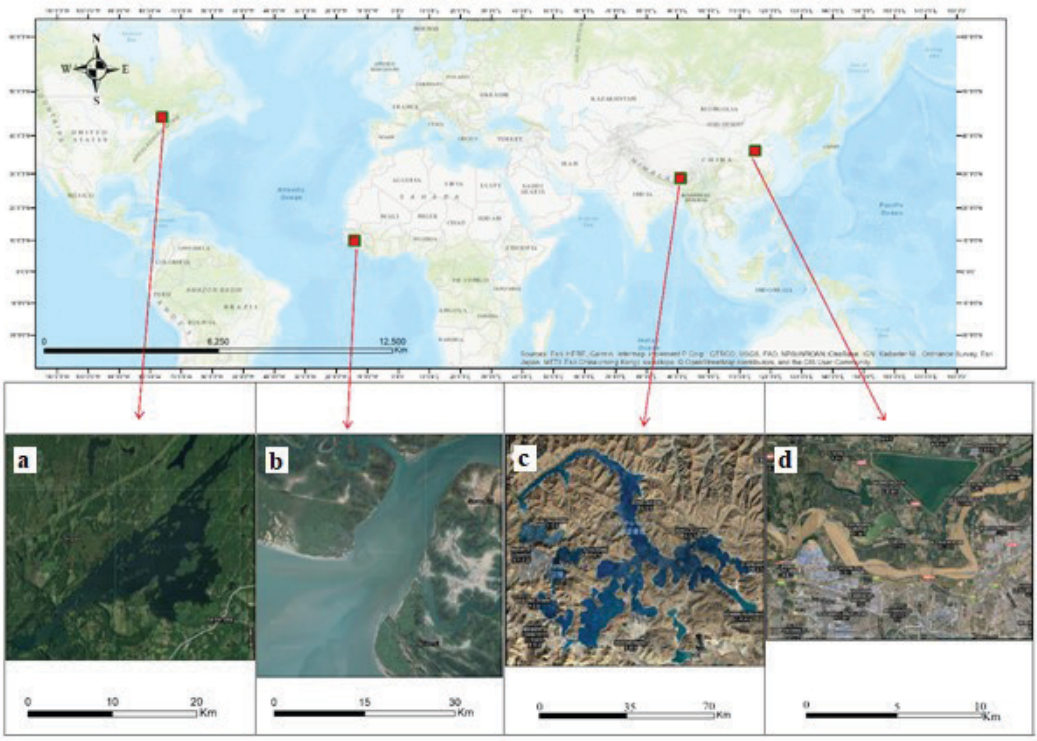

Figure 1: Study Areas a) Loughborough,Canada b)Dangara, Guinea d) Yamzho Yumco –Tibetan,China d) Yellow River Zhengzhou,China

The first study area is Loughborough Lake, located in the Cataraqui River basin, 20 km north of Kingston, Canada. The size of Loughborough Lake is 2002.9 hectares. The lake is divided into two main basins with very different characteristics. The western basin is on limestone, is much deeper (maximum 38.4m), is colder and contains species such as trout. The eastern basin is on the Canadian Shield and is shallower (maximum 7.6m) and warmer, with many islands and shallows. Like most lakes in the Cataraqui region, Lake Loughborough mixes in spring and autumn as the lake water warms and cools. During mixing, nutrients are cycled throughout the lake and it may appear cloudy with a brown or green colour from algae using cyclic nutrients. The water temperature varies according to depth (Gehrke, 2021).

The second image used in the study is Dangara in the Boke region on the Atlantic coast of Guinea. The Dangara inlet is located 20 km west of the Fatala Estuary. A tropical monsoon climate is dominant in the region. The length of the Dangara branch is 30 km, and the width of its mouth is 1 km. The shores are covered with rhizophoraceae mangroves. The bottom is covered with mud. Seasonal flow variations are not very evident in Dangara. Fresh water inflow is minimal and marine influence is dominant (Baran, 1995).

The third image used in the study is Yamzho Yumco Lake, located in the fault basin of southern Tibet. The altitude of the lake surface is 4441m. The lake is branch-shaped, extending northwest to southeast, with a maximum length of 74 km, a maximum width of 33 km and an average width of 8.62 km. The structural lake contains brackish water. The lake is quite meandering, with many major branches, he-

adlands and bays. There are many islands and islets in the lake with a total area of 44 km^2, the largest of which is 16.8 km^2 (Shao et al., 2008).

The last image is the Yellow River, located in the Zhengzhou district in Yellow River, China. In Zhengzhou the climate is warm, temperate, continental and monsoon, with four distinct seasons. The selected image has urban areas, water bodies, mostly turbid rivers (Yellow River), artificial channels, artificial lakes, reservoirs and ponds (Zhang et al., 2019).

2.3 Methods

The proposed method for automatic mapping of water bodies is given in Figure 2. The method has three stages: creation of the training pool and the training stage; image pre-processing stage; and classification stage. All operations in the method are carried out in the Google Earth Engine.

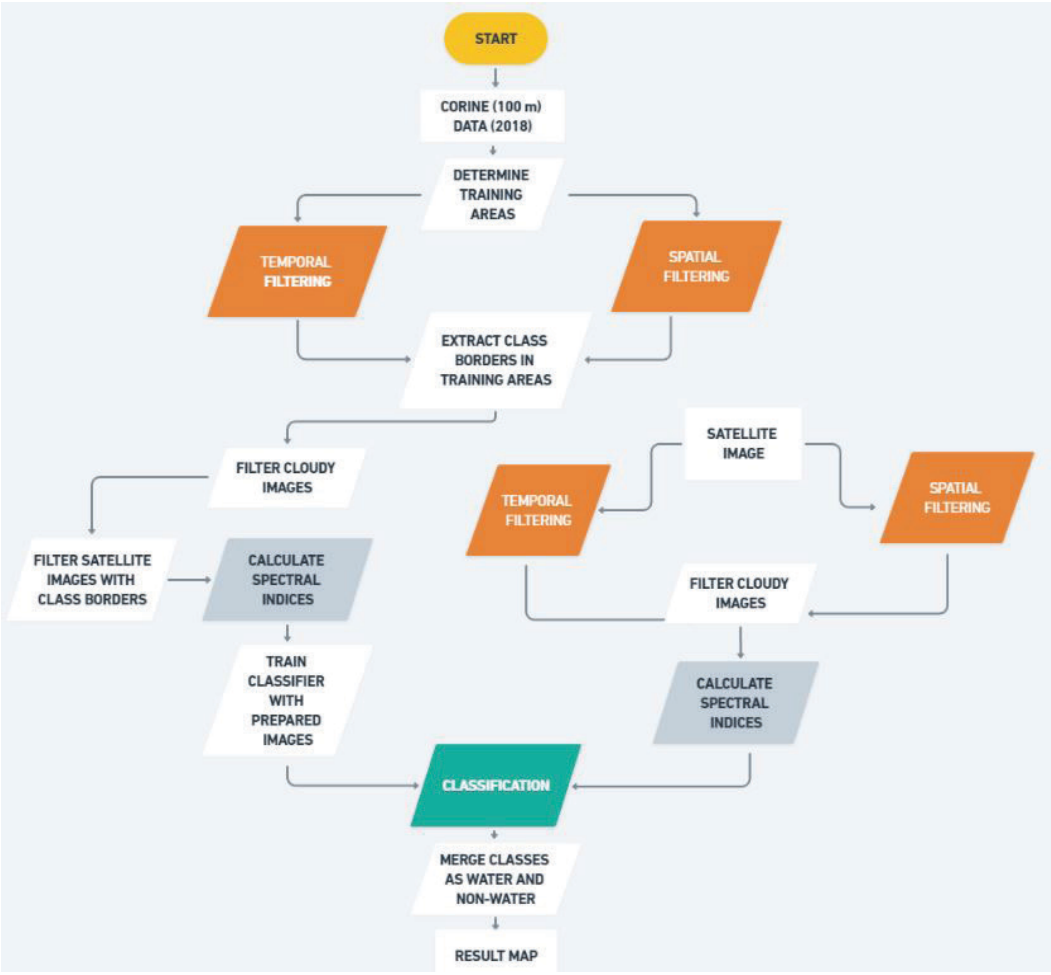

Figure 2: Workflow of the Proposed Method

One factor that directly affects the accuracy of the classification process is the training data (Foody ve Mathur, 2004). Therefore, creating a strong training dataset is critical, which is why the training regions are chosen (Table 2). After filtering the Corine data of the areas, the land classes were determined, and the boundaries of these areas were vectorised. In the training phase of the algorithm all of the Corine classes are used. Ones the class borders are extracted from the Corine image, classes which had the id of 511 (Water courses), 512 (Water bodies), 521 (Coastal lagoons),522 (Estuaries) and 523 (Sea and ocean) were grouped into water class. All remaining classes were grouped into the non-water class. Due to the resolution difference between the Corine data and Landsat data, a negative buffer of 200 m was applied, in order to get rid of the mixed classes at the edges of the Corine data (Figure 3).

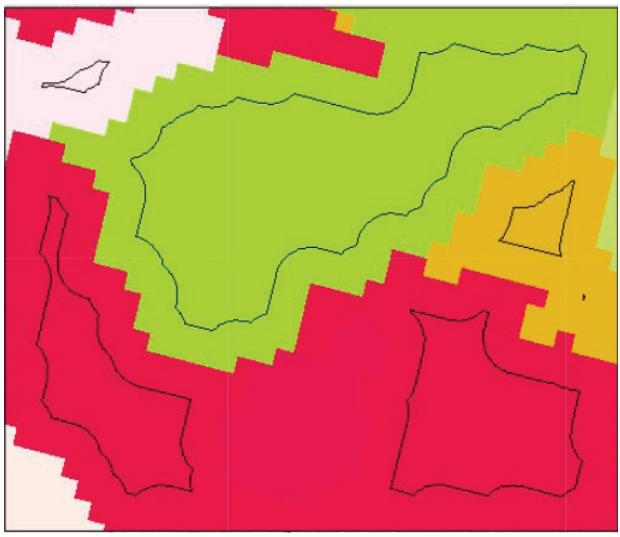

Figure 3: Created polygons from the Corine Data

Training data have been prepared in order to give successful results for water areas with different characteristics. The inclusion of classes found in the Corine data was accepted as a criterion when selecting the samples. In addition, versions of the same class in different geographies were also selected. Samples from Turkey, England, Greece, France and Sweden were selected as training data. Some of the selected sample regions are given in Figure 4.

At the end of the first stage, the satellite images in the training pool were filtered temporally and spatially. The average of the images for the year containing the test date is taken as the training data. Because there are too many cloud problems in optical images. In addition, it is necessary to take into account the periodic changes of classes. For the test images, the mean of the images belonging to October 2021 was used in this study.

Then the cloud images were removed from the pool. The spectral indices were calculated and included in the training data in order to increase the classification accuracy. The spectral indexes NDVI, NDWI, MNDWI-1, MNDWI-2, $AWEI_{sh}$ and $AWEI_{nsh}$ were used (Table 3).

Figure 4: Training Areas a) Samples from the water bodies b) Samples from the other classes

Table 3: Indices used in the study

Index	Name	Band math	Feature extraction	Reference
NDVI	Modified Normalized Difference Vegetation Index	$NDVI = \frac{NIR - RED}{NIR + RED}$	Vegetation extraction	(DeFries and Townshend, 1994)
NDWI	Modified Normalized Difference Water Index	$NDWI = \frac{GREEN - NIR}{GREEN + NIR}$	Identifies water components from satellite images	(Gao, 1996; McFeeters, 1996)
MNDWI-1	Modified Normalized Difference Water Index- 1	$MNDWI - 1 = \frac{GREEN - SWIR1}{GREEN + SWIR1}$	Aims to separate water from the background	(Xu, 2006)
MNDWI-2	Modified Normalized Difference Water Index-2	$MNDWI - 2 = \frac{GREEN - SWIR2}{GREEN + SWIR2}$	Aims to detect very low reflectance values for water features, shallow water and water with other features in the image	(Xu, 2006)
$AWEI_{sh}$	Automated Water Extraction Index-Shadow	$AWEIsh = BLUE + 2.5 \times Green$ $-1.5 \times (NIR + SWIR1) - 0.25 \times SWIR2$	Effectively eliminates non-water pixels, including dark surfaces, in areas with urban backgrounds	(Feyisa et al., 2014)
$AWEI_{nsh}$	Automated Water Extraction Index-Non Shadow	$AWEInsh = 4 \times (Green \times SWIR1) -$ $(0.25 \times NIR + 2.75 \times SWIR1)$	Improves the accuracy by removing shadow pixels that AWEIsh cannot effectively remove	(Feyisa et al., 2014)

After calculating spectral index values, the last step of the first stage was to filter the satellite images using the class boundaries obtained. Thus, the training pixels of the classes were determined. In the second stage of the proposed method, the satellite images were filtered temporally and spatially. Then, cloudy images were removed according to the Cloud rate data. In this study, images with a cloud cover of less than 0.5%, for training images and less than 10% for test images were selected. Then, the spectral indices were calculated. In the last stage, classification was carried out with the random forest algorithm. This algorithm has been preferred due to its ease of use and high accuracy rates in the literature.

The Random Forest classification algorithm is a machine learning method based on decision trees. Instead of branching each node using the best branch among all variables, RO branches each node using the randomly selected best variables at each node. Each dataset is generated by displacement from the original dataset. Trees are then developed using random feature selection. RO is also very fast, resistant to overfitting, and the the number of trees to work with can be adjusted (Breiman, 2001).

The results obtained were compared with the results obtained by K-means and Learning Vector Quantization (LVQ) methods. K-Means is one of the most preferred clustering algorithms. Clustering of data with statistically similar characteristics was performed. While performing clustering operations, separations are made so that a data is a member of only one cluster. The main purpose of the algorithm is to ensure that each cluster from the "K" clusters to be created is as different from each other as possible, so that the data of each cluster is close to each other (Hartigan and Wong, 1979).

The LVQ model is an artificial neural network model with a supportive learning strategy. Unlike the supervised learning strategy, both the input values and the expected output values are not given to the network for training in the supportive learning strategy. It only tells the LVQ network whether the output values produced for the input values are true or false. In the LVQ model, the goal is to represent a multi-dimensional vector with a set of vectors. That is, to represent a vector with a certain number of vectors. During training, the network determines with which vector set the input vectors will be expressed (Ito and Omatu, 1999; Kohonen, 1995). Accordingly, the number of classes for K-means was determined as 2. For LVQ, the number of classes = 2, the learning rate = 0.1 and the epoch value of 100 were used.

The accuracy of the classification results obtained was determined by the overall accuracy and kappa methods. One of the most commonly used metrics to evaluate the performance of classification results is overall accuracy. This value is calculated over the error matrix, where the estimates of the target attribute and the actual values are compared (Alberg et al., 2004). Kappa is a measure of how well the classifier actually performs. In other words, a model will have a high Kappa score if there is a large difference between accuracy and null error rate. Kappa can take a value between -1 and +1. A Kappa value of +1 indicates perfect agreement between the two observers, while a value of -1 indicates perfect discord between the two observers. If the kappa value is found to be 0, it indicates that the agreement between the two observers is not different from the agreement that may be due to chance (Kraemer, 2014).

3 RESULTS AND DISCUSSION

In order to test the proposed method, the images of water bodies in Canada, Tibetan, China and Guinea were classified. In order to assess the classification accuracy, 110 points for Canada, 100 points for Guinea and 125 points for Tibetan were created randomly using the high-resolution data available from Google Earth (Figure 5). The obtained results were compared with the K-Means and LVQ methods, which are frequently used in the unsupervised classification of remote sensing images.

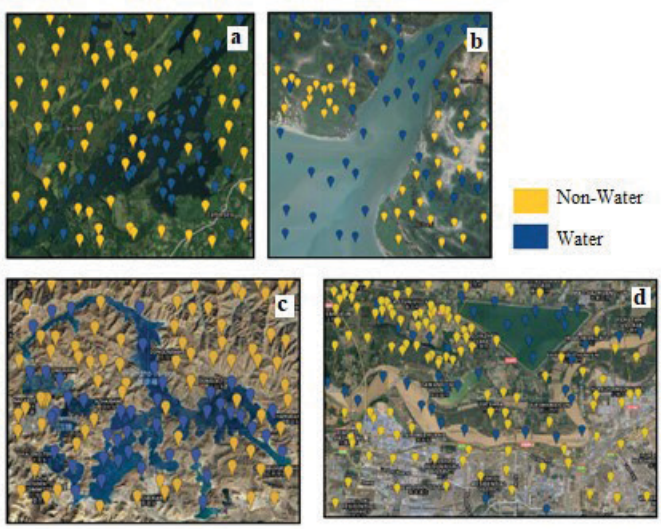

Figure 5: Points used for accuracy assessment

In order to test the proposed method, the various study areas with different geographies from around the world are used, the first of which is the region in Canada. The classification results are given in Figure 6.

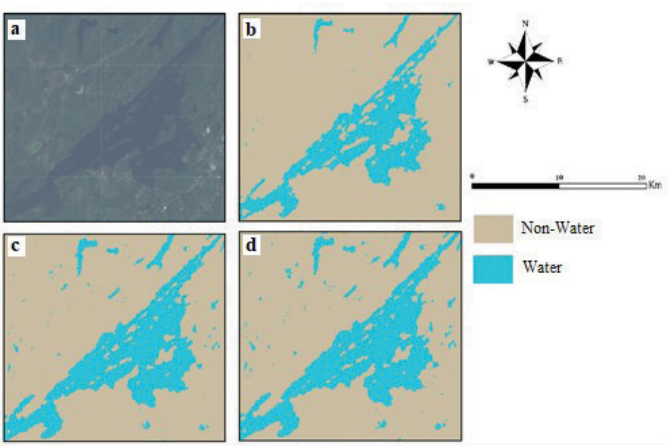

Figure 6: Classification Results for Canada Region a) Landsat Image b) Result of Proposed Algorithm c) Result of K-means d) Result of LVQ

To test the accuracy of the algorithm, the overall accuracy processed and kappa values are calculated. The results are given in Table 4, Table 5. Table 6, Table 7 respectively.

Table 4: Accuracy rates of obtained results

Method	Overall Accuracy	Kappa
Proposed Algorithm	0.94	0.87
LVQ	0.92	0.83
K-Means	0.92	0.83

The second classification process is carried out on the images of the Tibetan region. The classification results are given in Figure 7.

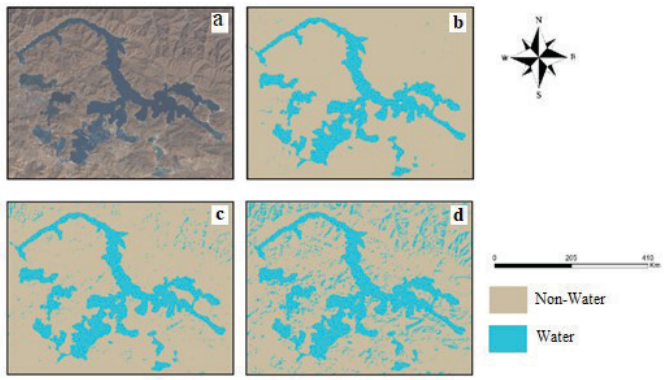

Figure 7: Classification Results for Guinea Region a) Landsat Image b) Result of Proposed Algorithm c) Result of K-means d) Result of LVQ

Table 5: Accuracy rates of obtained results for Guinea Region

Method	Overall Accuracy	Kappa
Proposed Algorithm	0.97	0.93
LVQ	0.92	0.84
K-Means	0.92	0.86

A third classification process is carried out on the images of the Tibetan region. Results are given in Figure 8.

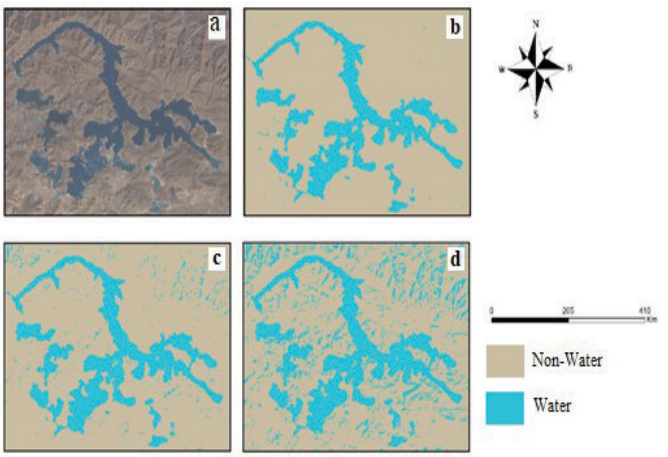

Figure 8: Classification Results for Tibetan Region a) Landsat Image b) Result of Proposed Algorithm c) Result of K-means d) Result of LVQ

Table 6: Accuracy rates of obtained results for Tibetan Region

Method	Overall Accuracy	Kappa
Proposed Algorithm	0.98	0.97
LVQ	0.82	0.66
K-Means	0.9	0.78

The last classification process is carried out on the images of the Zhengzhou region. Results are given in Figure 9

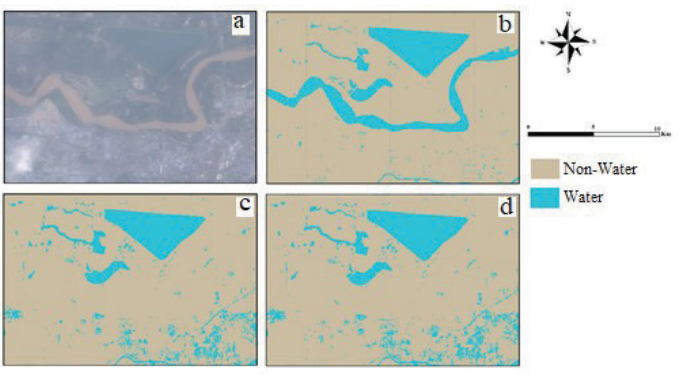

Figure 9: Classification Results for Zhengzhou Region a) Landsat Image b) Result of Proposed Algorithm c) Result of K-means d) Result of LVQ

Table 7: Accuracy rates of obtained results for Zhengzhou Region

Method	Overall Accuracy	Kappa
Proposed Algorithm	0.97	0.92
LVQ	0.83	0.53
K-Means	0.83	0.52

A new automatic water body extraction algorithm has been proposed in this study. The results were compared with other automatic classification methods, and the accuracy was higher. One of the biggest advantages of the proposed method is that it does not require any parameter or threshold values. It can work all over the world with a single training dataset. The methods used in the literature require either a parameter for classification or a specified threshold (Behnamian et al., 2017; Das et al., 2021). For example, a study using OpenStreetMap to remove water requires a filtering threshold to be determined (Zhang et al., 2019).

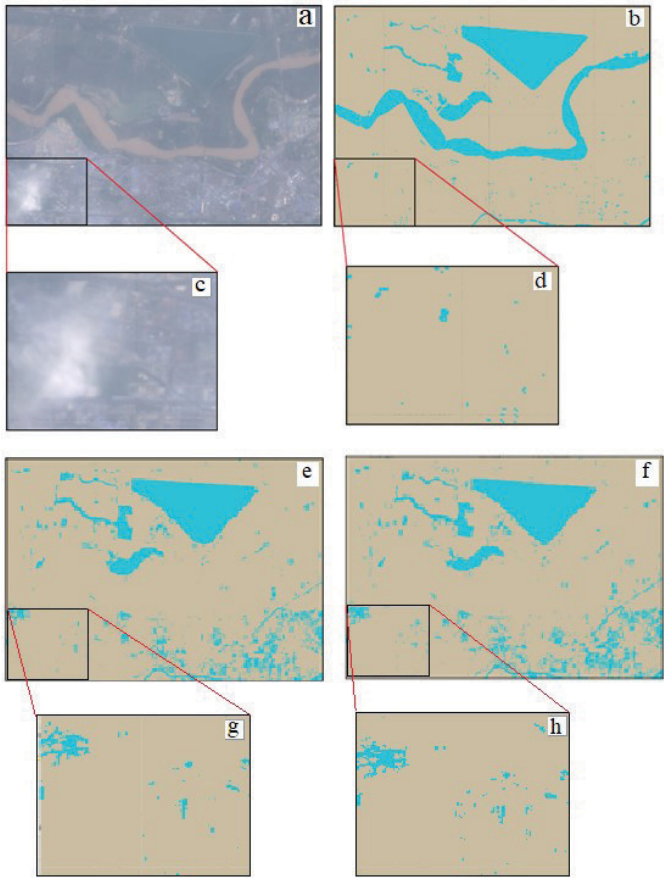

Figure 10: Classification Results for Zhengzhou Region a) Landsat Image b) Result of Proposed Algorithm c) Cloudy regions of the satellite image d) Classification results obtained by proposed algorithm e) Result of K-means f) Result of LVQ g) Classification results obtained by K-means h) Classification results obtained by LVQ

Another advantage of the proposed method is that it is not specific to any study area such as a city, mountainous region, plant, etc. In the Yellow River area used in this study, bare surfaces, urban area and turbid waters make water surface removal difficult. However, with the proposed method, various types of water area in the image are extracted successfully.

One of the biggest problems encountered in the extraction of water bodies is the presence of cloud-like noise in images. There is cloud in the image of the Zhengzhou area used in this study, but the results obtained with the proposed method show that it is much less affected by cloud than other methods (Figure 10).

In the literature, water extraction methods are usually prepared for a single type of water body, such as a lake, river, etc. (Jin et al., 2021; Nugraha et al., 2018; Xu et al., 2021). The results show that the proposed method can successfully extract various types of water body from the Landsat Images.

4 CONCLUSIONS

Water bodies play an important role in the life of living things and socioeconomic development. Therefore, any changes or developments should be monitored. Rapidly developing remote sensing technology offers opportunities for automatic extraction and dynamic monitoring of surface water bodies. However, these images need to be analysed accurately and quickly.

This study proposes an automated method of surface water extraction using Landsat 8 images and Corine data, which are used to prepare the training data. Once prepared, the training data can be used all over the world. The method gives successful results compared to other automatic classification methods used in the literature. The results show that the proposed method can be used successfully for water body extraction and monitoring.

In future studies, the success of the proposed method on images with different resolutions will be tested. For this purpose, satellite images such as Sentinel-2 and Planetscope will be used.

Literature and references

Alberg, A.J., Park, J.W., Hager, B.W., Brock, M.V., Diener-West, M., 2004. The use of "overall accuracy" to evaluate the validity of screening or diagnostic tests. Journal of general internal medicine, 19(5p1): 460-465.

Baran, E., 1995. Dynamique spatio-temporelle des peuplements de poissons estuariens en Guinée: Relations avec le milieu abiotique.

Behnamian, A. et al., 2017. Semi-automated surface water detection with synthetic aperture radar data: A wetland case study. Remote Sensing, 9(12): 1209.

Breiman, L., 2001. Random forests. Machine learning, 45(1): 5-32.

Chen, J., Du, P., Wu, C., Xia, J., Chanussot, J., 2018. Mapping urban land cover of a large area using multiple sensors multiple features. Remote Sensing, 10(6): 872.

Chen, Y., Tang, L., Kan, Z., Bilal, M., Li, Q., 2020. A novel water body extraction neural network (WBE-NN) for optical high-resolution multispectral imagery. Journal of Hydrology, 588: 125092.

Corine, 2019. CLC 2018 Copernicus Land Monitoring Service.

Dabija, A. et al., 2021. Comparison of support vector machines and random forests for corine land cover mapping. Remote Sensing, 13(4): 777.

Das, N. et al., 2021. Time series analysis of automated surface water extraction and thermal pattern variation over the Betwa river, India. Advances in Space Research, 68(4): 1761-1788.

DeFries, R.S., Townshend, J., 1994. NDVI-derived land cover classifications at a global scale. International Journal of Remote Sensing, 15(17): 3567-3586.

Dzieszko, P., 2014. Land-cover modelling using corine land cover data and multi-layer perceptron.

Feng, M., Sexton, J.O., Channan, S., Townshend, J.R., 2016. A global, high-resolution (30-m) inland water body dataset for 2000: first results of a topographic–spectral classification algorithm. International Journal of Digital Earth, 9(2): 113-133.

Feyisa, G.L., Meilby, H., Fensholt, R., Proud, S.R., 2014. Automated Water Extraction Index: A new technique for surface water mapping using Landsat imagery.

Remote Sensing of Environment, 140: 23-35.

Foody, G.M., Mathur, A., 2004. A relative evaluation of multiclass image classification by support vector machines. Ieee T Geosci Remote, 42(6): 1335-1343.

Franczyk, J., Chang, H., 2009. The effects of climate change and urbanization on the runoff of the Rock Creek basin in the Portland metropolitan area, Oregon, USA. Hydrological Processes: An International Journal, 23(6): 805-815.

Gallego, J., Peedell, S., 2001. Using CORINE Land Cover to map population density. Towards Agri-environmental indicators, Topic report, 6(2001): 92-103.

Gao, B.-C., 1996. NDWI—A normalized difference water index for remote sensing of vegetation liquid water from space. Remote sensing of environment, 58(3): 257-266.

Gao, H., Wang, L., Jing, L., Xu, J., 2016. An effective modified water extraction method for Landsat-8 OLI imagery of mountainous plateau regions, IOP conference series: earth and environmental science. IOP Publishing, pp. 012010.

Gehrke, T., 2021. MODELING SPECIES ABUNDANCE WITH IMPERFECT DETECTION USING ANGLING.

Hartigan, J.A., Wong, M.A., 1979. Algorithm AS 136: A k-means clustering algorithm. Journal of the Royal Statistical Society. Series C (Applied Statistics), 28(1): 100-108.

Hooshyar, M., Wang, D., Kim, S., Medeiros, S.C., Hagen, S.C., 2016. Valley and channel networks extraction based on local topographic curvature and k-means clustering of contours. Water Resources Research, 52(10): 8081-8102.

Huang, X., Xie, C., Fang, X., Zhang, L., 2015. Combining pixel-and object-based machine learning for identification of water-body types from urban high-resolution remote-sensing imagery. IEEE Journal of Selected Topics in Applied Earth Observations and Remote Sensing, 8(5): 2097-2110.

Huong, H.T.L., Pathirana, A., 2013. Urbanization and climate change impacts on future urban flooding in Can Tho city, Vietnam. Hydrology and Earth System Sciences, 17(1): 379-394.

Ito, Y., Omatu, S., 1999. Extended LVQ neural network approach to land cover mapping. Ieee T Geosci Remote, 37(1): 313-317.

Janssen, S., Dumont, G., Fierens, F., Mensink, C., 2008. Spatial interpolation of air pollution measurements using CORINE land cover data. Atmospheric Environment, 42(20): 4884-4903.

Jiang, W. et al., 2018. Multilayer perceptron neural network for surface water extraction in Landsat 8 OLI satellite images. Remote Sensing, 10(5): 755.

Jin, S. et al., 2021. River body extraction from sentinel-2A/B MSI images based on an adaptive multi-scale region growth method. Remote Sensing of Environment, 255: 112297.

Kohonen, T., 1995. Learning vector quantization, Self-organizing maps. Springer, pp. 175-189.

Kraemer, H.C., 2014. Kappa coefficient. Wiley StatsRef: statistics reference online: 1-4.

Kucsicsa, G. et al., 2019. Future land use/cover changes in Romania: regional simulations based on CLUE-S model and CORINE land cover database. Landscape and ecological engineering, 15(1): 75-90.

Matci, D.K., Avdan, U., 2020. Optimization-based automated unsupervised classification method: A novel approach. Expert Systems with Applications, 160: 113735.

McFeeters, S.K., 1996. The use of the Normalized Difference Water Index (NDWI) in the delineation of open water features. International journal of remote sensing, 17(7): 1425-1432.

McFeeters, S.K., 2013. Using the Normalized Difference Water Index (NDWI) within a Geographic Information System to Detect Swimming Pools for Mosquito Abatement: A Practical Approach. Remote Sensing, 5(7): 3544-3561.

Monegaglia, F., Zolezzi, G., Güneralp, I., Henshaw, A.J., Tubino, M., 2018. Automated extraction of meandering river morphodynamics from multitemporal remotely sensed data. Environmental Modelling & Software, 105: 171-186.

Nugraha, P.V.N., Wibirama, S., Hidayat, R., 2018. River body extraction and classification using enhanced models of modified normalized water difference index at Yeh Unda River Bali, 2018 International Conference on Information and Communications Technology (ICOIACT). IEEE, pp. 337-342.

Rad, A.M., Kreitler, J., Sadegh, M., 2021. Augmented Normalized Difference Water Index for improved surface water monitoring. Environmental Modelling & Software, 140: 105030.

Shao, Z. et al., 2008. Characteristics of the change of major lakes on the Qinghai-Tibet Plateau in the last 25 years. Frontiers of Earth Science in China, 2(3): 364-377.

Somasundaram, D. et al., 2020. Learning vector quantization neural network for surface water extraction from Landsat OLI images. J Appl Remote Sens, 14(3): 032605.

Stathopoulou, M., Cartalis, C., 2007. Daytime urban heat islands from Landsat ETM+ and Corine land cover data: An application to major cities in Greece. Solar Energy, 81(3): 358-368.

Waltner, I. et al., 2020. Spatial Assessment of the Effects of Land Cover Change on Soil Erosion in Hungary from 1990 to 2018. Isprs Int J Geo-Inf, 9(11): 667.

Wang, K., Zhu, Y., 2003. Recognition of water bodies from remotely sensed imagery by using neural network.

Xu, H., 2006. Modification of normalised difference water index (NDWI) to enhance open water features in remotely sensed imagery. International journal of remote sensing, 27(14): 3025-3033.

Xu, Y., Lin, J., Zhao, J., Zhu, X., 2021. New method improves extraction accuracy of lake water bodies in Central Asia. Journal of Hydrology: 127180.

Zhang, Z. et al., 2019. Automated surface water extraction combining Sentinel-2 imagery and openstreetmap using presence and background learning (PBL) algorithm. IEEE Journal of Selected Topics in Applied Earth Observations and Remote Sensing, 12(10): 3784-3798.

Matcı D. K. (2022). Automatic Delineation of Water Bodies Using Corine Data from Remotely Sensed Images.
Geodetski vestnik, 66 (3), 387-402.
DOI: https://doi.org/10.15292/geodetski-vestnik.2022.03.387-402

Dr. Dilek Küçük Matcı
Institute of Earth and Space Sciences, Eskişehir Technical University
Iki Eylul Campus, 26470, Eskisehir / TURKEY
e-mail: dkmatci@anadolu.edu.tr